NANO LETTERS

Letter

pubs.acs.org/NanoLett

Dynamic Control over the Optical Transmission of Nanoscale Dielectric Metasurface by Alkali Vapors

Jonathan Bar-David, Liron Stern, and Uriel Levy*

Department of Applied Physics, The Benin School of Engineering and Computer Science, The Center for Nanoscience and Nanotechnology, The Hebrew University of Jerusalem, Jerusalem, 91904, Israel

Supporting Information

ABSTRACT: In recent years, dielectric and metallic nanoscale metasurfaces are attracting growing attention and are being used for variety of applications. Resulting from the ability to introduce abrupt changes in optical properties at nanoscale dimensions, metasurfaces enable unprecedented control over light's different degrees of freedom, in an essentially two-dimensional configuration. Yet, the dynamic control over metasurface properties still remains one of the ultimate goals of this field. Here, we demonstrate the optical resonant interaction between a form birefringent dielectric metasurface made of silicon and alkali atomic vapor to control and effectively tune the optical transmission pattern initially generated by the nanoscale dielectric metasurface. By doing so, we present a controllable metasurface system, the output of which may be altered by applying magnetic fields, changing input polarization, or shifting the optical frequency. Furthermore, we also demonstrate the nonlinear behavior of our system taking advantage of the saturation effect of atomic transition. The demonstrated approach paves the way for using metasurfaces in applications where dynamic tunability of the metasurface is in need, for example, for scanning systems, tunable focusing, real time displays, and more.

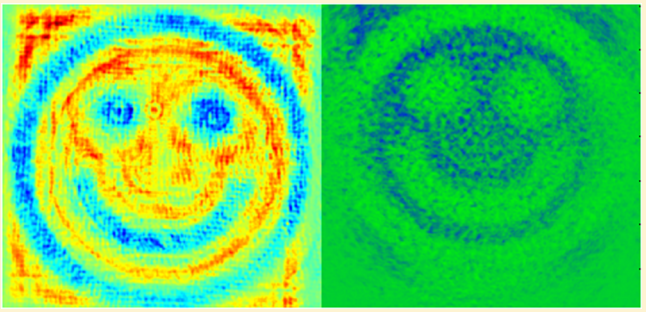

KEYWORDS: *dielectric metasurface, tunable metasurface, polarization encoding, photon-atom interaction*

Researchers in the field of nanophotonics have ever tried to manipulate light by interaction with nanostructures and consequently to control the patterns formed in the far-field. The emergence of the field of metasurfaces, consisting of nanopatterned interfaces and their resultant engineered refractive index,[1−14] enables the unprecedented nanoscale manipulation of the light's amplitude, phase, and polarization.[15−17]

The ability to design and fabricate ultrathin interfaces with an arbitrary refractive index at various wavelengths opens countless possibilities of manipulating light using nanoscale and near-field phenomena, and indeed metasurfaces have been suggested for multiple tasks including holograms of different kinds, polarization control, and other optical elements in both linear and nonlinear regimes.[15,17−25] To date, much of the metasurfaces demonstrated have included metallic gratings or structures.[26,27] The use of metals, although beneficial for phenomena such as field enhancement and surface waves, is not favorable for high-efficiency transmission type metasurfaces due to ohmic losses and interband transition absorption at visible and NIR wavelengths.[28,29] For these reasons, recently there has been great interest in dielectric metasurfaces, which for some applications may surpass the capabilities of metallic counterparts.[3−5,30−37]

The frontier of current research in the field of dielectric metasurfaces is the ability to actively control or tune the metasurfaces. Recent demonstrations based on free carrier plasma effect show promise,[38−41] yet the refractive index change is typically limited to the infrared regime and it is very difficult to achieve a significant modulation. To fill this void, we hereby propose and demonstrate a new paradigm in tunable metasurfaces using the optical resonant interaction between the electromagnetic field distribution created by the metasurface and alkali atomic vapor.

Alkali vapor cells are highly versatile physical systems in which multiple physical phenomena have been demonstrated, including dispersion control,[42] circular dichroism and birefringence,[43,44] wavelength conversion,[45] and electromagnetic induced transparency (EIT),[46] to name a few. Recently, some of these phenomena have been also demonstrated in compact, integrated photonic and plasmonic systems, where light-vapor interaction takes place via the evanescent part of the optical modes.[47−49]

Following the general trend for miniaturization and the fundamental interest in studying light-matter interactions in the nanoscale, a variety of systems have been demonstrated in which the interaction between vapor and light is confined to the nanoscale regime. Notable examples include the interaction of

Received: November 12, 2016
Revised: January 25, 2017
Published: January 26, 2017

DOI: 10.1021/acs.nanolett.6b04740
Nano Lett. 2017, 17, 1127−1131

light reflected from a boundary between a dielectric and vapor,[50] the guided wave evanescent interactions in chip-scale systems,[47,49,51] and the plasmonic atomic hybrid modes.[48,52,53] In this work, we use a rubidium (Rb) vapor cell to obtain dynamic control over the transmission of a designed metasurface by tuning their combined behavior. To achieve this, we alter the polarization profile of transmitted light, rather than its amplitude profile (as a normal image would). As a result, we can actively control the intensity distribution of the electromagnetic field transmitted from the nanoscale dielectric metasurface by exploiting the dichroism in the alkali vapor cell. This allows for applications such as tunable display, tunable focusing, active scanners and parallel communications devices to be mitigated using metasurface technology.

Device Design, Fabrication, and Concept of Operation. Subwavelength gratings are known to exhibit strong, artificial birefringence due to the difference in the continuity condition of the electric and displacement fields ($\vec{E}$ and $\vec{D}$, respectively) across different media for TM and TE polarizations,[3,54−57] as illustrated in Figure 1a. The effective

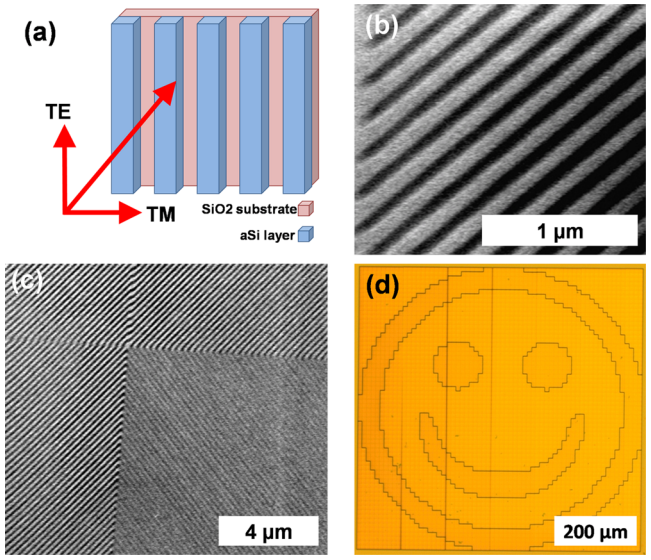

Figure 1. (a) Illustration of a nanoscale grating with the associated polarization directions. (b) Scanning electron microscope (SEM) micrograph showing a part of a single 10 × 10 μm pixel. (c) SEM micrograph, corner of four adjacent pixels of the fabricated metasurface. (d) Microscope image of the whole metasurface.

medium[57] approach (EMT) allows one to calculate the effective refractive index for transverse electric (TE) and transverse magnetic (TM) polarizations, respectively, by a set of two simple equations

$$n_{TE} = \sqrt{f n_1^2 + (1-f) n_2^2} \quad (1)$$

$$n_{TM} = \frac{n_1 n_2}{\sqrt{f n_2^2 + (1-f) n_1^2}} \quad (2)$$

where n_{TE} and n_{TM} are the effective indices for TE and TM polarizations, respectively, f is the period fill factor, and n_1 and n_2 are the bulk refractive indices of the two materials of which the structure is made.

By using this approach, one may design and fabricate ultrathin nanoscale metasurfaces with strong artificial birefringence and use them to spatially control the transmitted light through an interface in what may be called a polarization-controlling metasurface.[3,17,19,57]

The above-mentioned effective-medium approach was used to design and fabricate a metasurface that acts as a quarter-wave plate (QWP), converting linearly polarized light to left- or right-handed circular polarized light (LHCP or RHCP, respectively), depending on the orientation of the structure. It should be noted that the EMT was also validated by full wave simulation (see Supporting Information). The metasurface is made of a 175 nm thick amorphous silicon (a-Si) layer, in which is embedded a grating with a period of 200 nm, and fill-factor of 0.45, corresponding to a 90 nm line-width. To create a recognizable image, we have defined two basic metasurface pixels in which the nanoscale pattern is rotated at an angle of ±45° with respect to the vertical axis of the image. Figure 1a depicts the basic structure concept while Figure 1b,c presents scanning electron microscope (SEM) micrographs of the subwavelength grating structure and the boundary between two different pixels, respectively. For linearly polarized light, each basic pixel acts as a local QWP, converting the incident linearly polarized light to RHCP or LHCP light, respectively. The 64-by-64 such basic pixels were placed together to form an array with the desired "smiley" image, shown in Figure 1d. Note that the information is in the polarization domain, unlike typical metasurfaces in which the information is encoded by phase or amplitude modulation. The actual fabrication of this design involves plasma enhanced chemical vapor deposition (PECVD, Oxford) of a 175 nm thick layer of amorphous silicon (a-Si) on a glass substrate, followed by defining LHCP or RHCP pixels via E-beam lithography (Raith Eline). Finally, the pattern was transferred into the a-Si layer by reactive ion etching (RIE, Corial).

Next, one needs to consider the interaction of light emanating from the metasurface with the atomic vapor medium. Here we consider the absorption of Rb^{85} vapor at the D1 transition at the wavelength of 795 nm, associated with the $5^2S_{1/2} \rightarrow 5^2P_{1/2}$ electronic transition.[58] Energy levels splitting associated with this absorption line occurs by applying a direct current (dc) magnetic field and is known to generate strong circular-polarization birefringence and dichroism.[43] In this work, we use this feature of Rb vapor to provide dynamic tunability and to modulate the transmission properties of our metasurface.

Optical Characterization of Nanoscale Polarization Metasurface. The optical setup used for the characterization of our metasurface before interacting with the Rb vapor is illustrated in Figure 2a. Its aim is to measure the Stokes parameters generated by the metasurface device. The information on a "smiley" face was encoded by our metasurface as a circular polarization distribution. Indeed, the transmitted image from the "smiley" polarization pattern is nearly undetectable by conventional imaging setup, as it is the pixels that differ in polarization rather than in the transmitted amplitude. However, the image is well observed by examining the Stokes parameters of transmitted light at the image plane, as may be seen in Figure 2b, which presents the measurement results of the S_3 stokes parameter. One can clearly notice the circular polarization distribution created by our metasurface. It is worth noting that while the smiley image in Figure 1d contains polarization information, it is still visible due to the use of a microscope in reflection mode, with a broad illumination spectrum and an NA much higher than that of a collimated laser beam as used for Stokes measurement. Yet, the visible

DOI: 10.1021/acs.nanolett.6b04740
Nano Lett. 2017, 17, 1127−1131

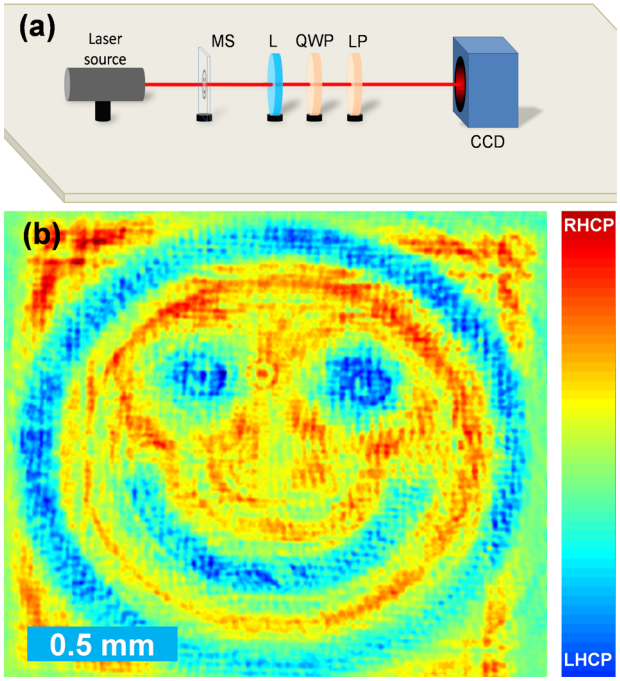

Figure 2. (a) Illustration of the setup used for optical characterization of our metasurface: MS, metasurface; L, lens; QWP, quarter waveplate; LP, linear polarizer. (b) Measured S3 Stokes parameter, clearly showing the encoding of information as circularly polarized light in the space domain. All experiments used a tunable laser at a wavelength of 795 nm.

lines in that image are the borders between different pixel types that are somewhat broader due to over exposure in fabrication process, while borders between similar pixels are barely visible.

Results. The experimental setup used to demonstrate the dynamic control of our combined Rb vapor-nanoscale metasurface system is depicted in Figure 3a. The "smiley" image is created on a charge-coupled device array by an imaging system where the Rb vapor cell is positioned in close proximity to the image plane. A coil wrapped around the Rb cell is used as an electromagnet to apply a dc magnetic field of ∼180 G in the Faraday configuration (i.e., in the light's propagation direction). All experiments were conducted at room temperature. Figure 3b shows the measured transmission spectrum from the Rb cell before being integrated into the metasurface setup. For this purpose, the Rb cell was subjected to a plane wave illumination around the Rb's resonant wavelength of 795 nm, spanning both F = 2 → F′ and F = 3 → F′ manifolds. The green curve corresponds to the measured spectroscopic result obtained with linearly polarized illumination and without the application of magnetic field, whereas the red and blue curves (for left and right handed circularly polarized light respectively) are the absorption spectra for the case where magnetic field is applied. These curves show the strong circular dichroism and are used to explain the operation concept of our system. Simply put, the transmission from the metasurface can be varied strongly by switching the polarization of light for a given magnetic field, or by controlling the magnetic field for a given polarization. Alternatively, one may use the wavelength degree of freedom and control the displayed image by frequency scanning.

Following the basic spectroscopy experiment, we next illuminate the 7.5 cm long Rb cell by the polarization pattern transmitted from our metasurface. The obtained results, shown

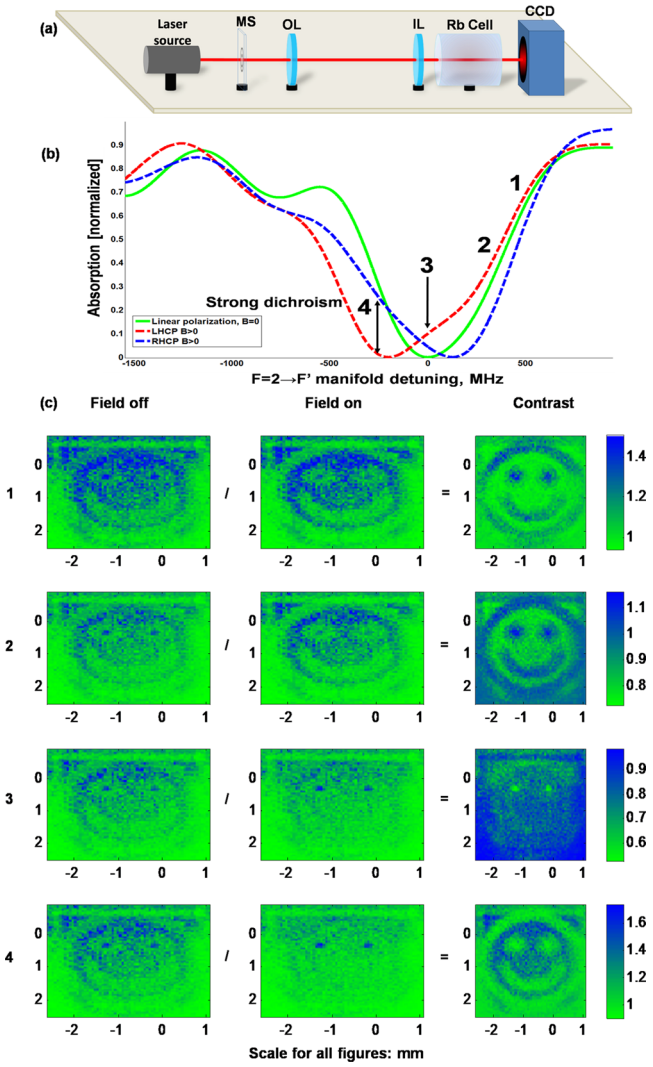

Figure 3. (a) Illustration of the optical control setup: MS, metasurface; OL, objective lens, f = 5 cm; IL, image lens, f = 25 cm; ∼10 cm long rubidium cell wrapped by an electromagnet. Metasurface illuminated by a tunable laser with wavelength of 795 nm. (b) Measurements of the Zeeman splitting of the Rb absorption lines, resulting in a circular dichroism in the Rb cell. The absorption is normalized and the true value is ∼30%. (c) Smiley images recorded with and without the magnetic field in the Rb cell. The contrast shows the ratio between the images recorded with and without the field and is normalized to the natural absorption at the same frequency. All images are presented with 10 × 10-pixel binning. Unbinned images are presented in the Supporting Information.

in Figure 3c, presents the transmitted image with (left column) and without (center column) the application of magnetic field. The contrast, given as the ratio between the two columns, is displayed in the right column. Each row in the figure was captured at a different frequency corresponding to the label presented in Figure 3b, green curve. As may be seen from our measurements, the best contrast is not obtained at resonance but rather at slightly off resonant frequencies where the dichroism brings the contrast between LHCP and RHCP to a maximum. Moreover, it is fairly clear that the contrast on opposite sides of the resonance is inverted, as is predicted from the absorption curves.[40]

Finally, we have tested the effect of rotating the incident light polarization from horizontal to vertical. The result of this

DOI: 10.1021/acs.nanolett.6b04740
Nano Lett. 2017, 17, 1127−1131

change (presented in Figure 4) is an inversion of the image contrast, which is a direct consequence of interchanging RHCP

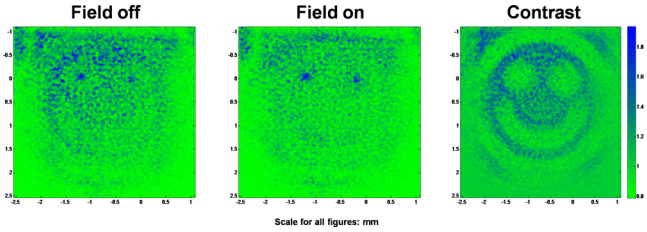

Figure 4. Measurement 0.4 GHz above the resonant frequency, with illumination polarization rotated by 90°. The measurement was done at a frequency similar to measurement 1 in Figure 3c. Yet, the result is inverted in contrast and resembles that of measurement 4 in Figure 3d. This is an evident for the equivalence between polarization rotation and frequency mirroring.

and LHCP. The result presented in Figure 4 was recorded with identical conditions to those which were used to capture the image in Figure 3c-2; however the captured image itself is nearly identical to that of detuning the frequency to the other side of the resonance, as may be seen by comparing Figure 4 to Figure 3c-4. This observation indicates that switching of incident polarization from RHCP to LHCP is equivalent to detuning the frequency from one side of the absorption resonance to the other.

One should also note that the Rb media is highly nonlinear, opening up some new avenues in nonlinear tunable metasurfaces. The nonlinear regime in the operation of this system is further discussed in the Supporting Information.

Conclusions. The ability to control and tune the properties of nanoscale metasurfaces in real time is a major challenge in metasurface research. In this work, we have demonstrated an atomic metasurface system by combining a form birefringent dielectric metasurface made of nanoscale silicon structures with alkali vapor (rubidium). This combined system allows one to actively control the transmission of light by altering the input polarization, the optical frequency, and the applied magnetic field. Unlike "conventional" metasurfaces, our device alters the spatial polarization rather than spatial amplitude (or phase) profile of the transmitted light, which allows us to control the image properties taking advantage of the strong circular dichroism of rubidium, serving as an optical element which converts light's polarization distribution into observable amplitude distribution. This experimental scheme may be further developed to be fully integrated on a chip, which should provide even better spatial resolution and may allow one to study the near-field interactions between the metasurface and rubidium vapor. Finally, the demonstrated approach can be used for variety of applications from tunable displays to tunable focusing, real time scanners, and parallel metasurface-based free space communication systems.

■ ASSOCIATED CONTENT

Supporting Information

The Supporting Information is available free of charge on the ACS Publications website at DOI: 10.1021/acs.nanolett.6b04740.

Validity of effective medium calculation, TE versus TM transmission, nonlinear effects - Rb saturation, and integration of a metasurface with a hot vapor thin cell (PDF)

■ AUTHOR INFORMATION

Corresponding Author

*E-mail: ulevy@mail.huji.ac.il.

ORCID

Jonathan Bar-David: 0000-0002-4464-636X

Uriel Levy: 0000-0002-5918-1876

Notes

The authors declare no competing financial interest.

■ ACKNOWLEDGMENTS

We acknowledge financial support from the ActiPlAnt program of the Einstein foundation, Berlin.

■ REFERENCES

(1) Yu, N.; Capasso, F. *Nat. Mater.* **2014**, *13* (2), 139−150.
(2) Shitrit, N.; Bretner, I.; Gorodetski, Y.; Kleiner, V.; Hasman, E. *Nano Lett.* **2011**, *11* (5), 2038−2042.
(3) Flanders, D. C. *Appl. Phys. Lett.* **1983**, *42* (6), 492−494.
(4) Lalanne, P.; Astilean, S.; Chavel, P.; Cambril, E.; Launois, H. *Opt. Lett.* **1998**, *23* (14), 1081−1083.
(5) Lalanne, P.; Astilean, S.; Chavel, P.; Cambril, E.; Launois, H. *J. Opt. Soc. Am. A* **1999**, *16* (5), 1143.
(6) Lin, D.; Fan, P.; Hasman, E.; Brongersma, M. L. *Science* **2014**, *345* (6194), 298−302.
(7) Ni, X.; Kildishev, A. V.; Shalaev, V. M. *Nat. Commun.* **2013**, *4*, 2807.
(8) Shalaev, M. I.; Sun, J.; Tsukernik, A.; Pandey, A.; Nikolskiy, K.; Litchinitser, N. M. *Nano Lett.* **2015**, *15* (9), 6261−6266.
(9) Pors, A.; Albrektsen, O.; Radko, I. P.; Bozhevolnyi, S. I. *Sci. Rep.* **2013**, *3*, 2155.
(10) Pors, A.; Nielsen, M. G.; Bozhevolnyi, S. I. *Nano Lett.* **2015**, *15* (1), 791−797.
(11) Bomzon, Z.; Biener, G.; Kleiner, V.; Hasman, E. *Opt. Lett.* **2002**, *27* (13), 1141.
(12) Hasman, E.; Kleiner, V.; Biener, G.; Niv, A. *Appl. Phys. Lett.* **2003**, *82* (3), 328−330.
(13) Levy, U.; Tsai, C.-H.; Pang, L.; Fainman, Y. *Opt. Lett.* **2004**, *29* (15), 1718−1720.
(14) Levy, U.; Kim, H.-C.; Tsai, C.-H.; Fainman, Y. *Opt. Lett.* **2005**, *30* (16), 2089−2091.
(15) Yifat, Y.; Eitan, M.; Iluz, Z.; Hanein, Y.; Boag, A.; Scheuer, J. *Nano Lett.* **2014**, DOI: 10.1021/nl5001696.
(16) Segal, N.; Keren-Zur, S.; Hendler, N.; Ellenbogen, T. *Nat. Photonics* **2015**, *9* (3), 180−184.
(17) Levy, U.; Kim, H.-C.; Tsai, C.-H.; Fainman, Y. *Opt. Lett.* **2005**, *30* (16), 2089−2091.
(18) Lerman, G. M.; Levy, U. *Opt. Lett.* **2008**, *33* (23), 2782−2784.
(19) Desiatov, B.; Mazurski, N.; Fainman, Y.; Levy, U. *Opt. Express* **2015**, *23* (17), 22611−22618.
(20) Clausen, J. S.; Højlund-Nielsen, E.; Christiansen, A. B.; Yazdi, S.; Grajower, M.; Taha, H.; Levy, U.; Kristensen, A.; Mortensen, N. A. *Nano Lett.* **2014**, *14* (8), 4499−4504.
(21) Zhu, X.; Vannahme, C.; Højlund-Nielsen, E.; Mortensen, N. A.; Kristensen, A. *Nat. Nanotechnol.* **2015**, *11* (4), 325−329.
(22) Kumar, K.; Duan, H.; Hegde, R. S.; Koh, S. C. W.; Wei, J. N.; Yang, J. K. W. *Nat. Nanotechnol.* **2012**, *7* (9), 557−561.
(23) Wen, D.; Chen, S.; Yue, F.; Chan, K.; Chen, M.; Ardron, M.; Li, K. F.; Wong, P. W. H.; Cheah, K. W.; Pun, E. Y. B.; Li, G.; Zhang, S.; Chen, X. *Adv. Opt. Mater.* **2016**, *4* (2), 321−327.
(24) Li, G.; Chen, S.; Pholchai, N.; Reineke, B.; Wong, P. W. H.; Pun, E. Y. B.; Cheah, K. W.; Zentgraf, T.; Zhang, S. *Nat. Mater.* **2015**, *14* (6), 607−612.
(25) Almeida, E.; Bitton, O.; Prior, Y. *Nat. Commun.* **2016**, *7*, 12533.
(26) Novotny, L.; van Hulst, N. *Nat. Photonics* **2011**, *5* (2), 83−90.
(27) Brener, I.; Miao, X.; Shaner, E. A.; Passmore, B. S.; Jun, Y. C. *Mid-infrared tunable metamaterials*. US9018642B1, April 28, 2015.

DOI: 10.1021/acs.nanolett.6b04740
Nano Lett. 2017, 17, 1127−1131

(28) Huang, Y.-W.; Chen, W. T.; Tsai, W.-Y.; Wu, P. C.; Wang, C.-M.; Sun, G.; Tsai, D. P. *Nano Lett.* **2015**, *15* (5), 3122−3127.
(29) Shrestha, V. R.; Lee, S.-S.; Kim, E.-S.; Choi, D.-Y. *Nano Lett.* **2014**, *14* (11), 6672−6678.
(30) Desiatov, B.; Mazurski, N.; Fainman, Y.; Levy, U. *Opt. Express* **2015**, *23* (17), 22611.
(31) Chong, K. E.; Hopkins, B.; Staude, I.; Miroshnichenko, A. E.; Dominguez, J.; Decker, M.; Neshev, D. N.; Brener, I.; Kivshar, Y. S. *Small* **2014**, *10* (10), 1985−1990.
(32) Decker, M.; Staude, I.; Falkner, M.; Dominguez, J.; Neshev, D. N.; Brener, I.; Pertsch, T.; Kivshar, Y. S. *Adv. Opt. Mater.* **2015**, *3* (6), 813−820.
(33) Evlyukhin, A. B.; Novikov, S. M.; Zywietz, U.; Eriksen, R. L.; Reinhardt, C.; Bozhevolnyi, S. I.; Chichkov, B. N. *Nano Lett.* **2012**, *12* (7), 3749−3755.
(34) Yu, Y. F.; Zhu, A. Y.; Paniagua-Domínguez, R.; Fu, Y. H.; Luk'yanchuk, B.; Kuznetsov, A. I. *Laser Photonics Rev.* **2015**, *9* (4), 412−418.
(35) Chong, K. E.; Staude, I.; James, A.; Dominguez, J.; Liu, S.; Campione, S.; Subramania, G. S.; Luk, T. S.; Decker, M.; Neshev, D. N.; Brener, I.; Kivshar, Y. S. *Nano Lett.* **2015**, *15* (8), 5369−5374.
(36) Evlyukhin, A. B.; Reinhardt, C.; Seidel, A.; Luk'yanchuk, B. S.; Chichkov, B. N. *Phys. Rev. B: Condens. Matter Mater. Phys.* **2010**, *82* (4), 045404.
(37) Kuznetsov, A. I.; Miroshnichenko, A. E.; Brongersma, M. L.; Kivshar, Y. S.; Luk'yanchuk, B. *Science* **2016**, *354* (6314), aag2472.
(38) Lewi, T.; Iyer, P. P.; Butakov, N. A.; Mikhailovsky, A. A.; Schuller, J. A. *Nano Lett.* **2015**, *15* (12), 8188−8193.
(39) Yao, Y.; Shankar, R.; Kats, M. A.; Song, Y.; Kong, J.; Loncar, M.; Capasso, F. *Nano Lett.* **2014**, *14* (11), 6526−6532.
(40) Lee, J.; Jung, S.; Chen, P.-Y.; Lu, F.; Demmerle, F.; Boehm, G.; Amann, M.-C.; Alù, A.; Belkin, M. A. *Adv. Opt. Mater.* **2014**, *2* (11), 1057−1063.
(41) Huang, Y.-W.; Lee, H. W. H.; Sokhoyan, R.; Pala, R. A.; Thyagarajan, K.; Han, S.; Tsai, D. P.; Atwater, H. A. *Nano Lett.* **2016**, *16* (9), 5319−5325.
(42) Hau, L. V.; Harris, S. E.; Dutton, Z.; Behroozi, C. H. *Nature* **1999**, *397* (6720), 594−598.
(43) Stern, L.; Szapiro, A.; Talker, E.; Levy, U. *Opt. Express* **2016**, *24* (5), 4834−4841.
(44) Weller, L.; Kleinbach, K. S.; Zentile, M. A.; Knappe, S.; Hughes, I. G.; Adams, C. S. *Opt. Lett.* **2012**, *37* (16), 3405−3407.
(45) Kienlen, M. B.; Holte, N. T.; Dassonville, H. A.; Dawes, A. M. C.; Iversen, K. D.; McLaughlin, R. M.; Mayer, S. K. *Am. J. Phys.* **2013**, *81* (6), 442−449.
(46) Boller, K.-J.; Imamoğlu, A.; Harris, S. E. *Phys. Rev. Lett.* **1991**, *66* (20), 2593−2596.
(47) Stern, L.; Levy, U. *Opt. Express* **2012**, *20* (27), 28082−28093.
(48) Stern, L.; Grajower, M.; Levy, U. *Nat. Commun.* **2014**, *5*, 4865.
(49) Stern, L.; Desiatov, B.; Goykhman, I.; Levy, U. *Nat. Commun.* **2013**, *4*, 1548.
(50) Briaudeau, S.; Bloch, D.; Ducloy, M. *EPL Europhys. Lett.* **1996**, *35* (5), 337.
(51) Ritter, R.; Gruhler, N.; Pernice, W.; Kübler, H.; Pfau, T.; Löw, R. 2015, ArXiv150500611 Phys. (Accessed Sep 25, 2016).
(52) Chan, E. A.; Aljunid, S. A.; Adamo, G.; Laliotis, A.; Ducloy, M.; Wilkowski, D. 2016, ArXiv160607990 Cond-Mat Physicsphysics. (Accessed Sep 25, 2016).
(53) Chan, E. A.; Aljunid, S. A.; Zheludev, N. I.; Wilkowski, D.; Ducloy, M. *Opt. Lett.* **2016**, *41* (9), 2005−2008.
(54) Born, M.; Wolf, E. *Principles of Optics: Electromagnetic Theory of Propagation, Interference and Diffraction of Light*; CUP Archive, **2000**.
(55) Yeh, P.; Yariv, A.; Hong, C.-S. *J. Opt. Soc. Am.* **1977**, *67* (4), 423−438.
(56) Yariv, A.; Yeh, P. *J. Opt. Soc. Am.* **1977**, *67* (4), 438−447.
(57) Rytov, S. M. *JETP* **1956**, *2* (3), 466.
(58) Steck, D. A. Rubidium 85 D Line Data, http://steck.us/alkalidata/ (accessed Apr 13, 2016).

DOI: 10.1021/acs.nanolett.6b04740
Nano Lett. 2017, 17, 1127−1131